Nitrogen-Doped Carbons with Hierarchical Porosity via Chemical Blowing Towards Long-Lived Metal-Free Catalysts for Acetylene Hydrochlorination

Selina K. Kaiser,[a] Kyung Seob Song,[b] Sharon Mitchell,[a] Ali Coskun,*[b] and Javier Pérez-Ramírez*[a]

Porous nitrogen-doped carbons (NCs) are sustainable alternatives to the toxic mercury-based acetylene hydrochlorination catalysts applied in the manufacture of polyvinyl chloride. However, the application of NCs as metal-free catalysts is hampered by their insufficient durability under industrially relevant process conditions. In particular, pore blockage leads to accelerated deactivation of NCs compared to the state-of-the-art precious metal-based systems. Herein, we develop a salt template-assisted synthesis strategy coupled with chemical blowing to tune the textural properties of NCs, while preserving the N-content and speciation. The addition of metal salts (*i.e.*, $Mg(OAc)_2$ or $CaCO_3$) enhances gas evolution, leading to an increased formation of micro- and mesopores, while the *in-situ* generated $CaO/CaCl_2$ and $MgO/MgCl_2$ develop auxiliary pore networks. Micropores are easily blocked during acetylene hydrochlorination, but meso- and macropores are structurally stable, enhancing the lifetime of hierarchical NCs by *ca.* 50 times compared to their non-templated analogues, rivaling the stability of benchmark metal-based catalysts.

Metal-free carbon materials have demonstrated considerable potential as sustainable catalysts for diverse applications, including clean energy generation and storage, and the production of bulk chemicals and commodities.[1] A prominent example is the manufacture of vinyl chloride monomer (VCM) *via* acetylene hydrochlorination, a key industrial technology (13 Mton y^{-1}), which runs over highly-toxic and volatile mercury-based catalysts, causing severe consequences for human health and the environment. In recent years, extensive research has been conducted on ruthenium- and especially gold-based systems,[5] leading in some cases to pilot plant demonstrations (*e.g.,* thiosulfate stabilized gold-based catalysts).[5b] Still, carbon materials, including defect-rich carbons,[2] graphitic carbon nitride,[3] and heteroatom-doped carbons (*i.e.*, N, P, B, S)[4] are highly desirable alternatives, owing to their significant environmental and cost advantages compared to metal-based catalysts.[5] In particular, nitrogen-doped carbons (NCs), derived *via* carbonization of C/N-precursors (*i.e.*, polyaniline,[4f] polydopamine,[6] ZIF-8[4d]), stand out as the most promising candidates, rivaling the initial activity of their metal-based analogues at elevated reaction temperatures.[4f,5d,e] Despite these encouraging results, the applicability of NCs is hindered by their insufficient durability under relevant process conditions (T = 403-453 K, P = 1.5 bar, $HCl:C_2H_2 = 1.1:1$).[4d,5c,d,7] In particular, pore blockage through the formation of carbonaceous residues has been identified as the major reason for catalyst deactivation.[4f,6] A possible strategy to mitigate the impact of coke species is to enhance the micropore volume and introduce auxiliary pores to improve the accessibility of the active sites within the micropores and facilitate the molecular diffusion of reactants, intermediates, and products.

Previous attempts in this direction were based on (*i*) varying the carbonization temperature[3b,4d,f,6] or (*ii*) using hard templates (*e.g.*, silica[4c,e,8] or metal organic frameworks[4b]). While high carbonization temperatures favor the formation of microporosity and high specific surface areas, the total N-content significantly decreases with rising temperature, which commonly leads to a lower catalytic activity. On the contrary, hard templates, although they do not significantly alter the N-content, mainly generate meso- and/or macropores, while their synthesis often involves costly precursors or hazardous purification steps (*e.g.* treatment in HF-solution). Recently, chemical blowing, which generates micropores during the carbonization process through gas evolution by decomposing ammonium chloride (NH_4Cl) into HCl and NH_3, was introduced as an alternative strategy to yield highly microporous NCs.[9] The possible combination of this approach with thermally decomposable templates, such as magnesium acetate ($Mg(OAc)_2$) or calcium carbonate ($CaCO_3$), could boost the chemical blowing effect and further introduce auxiliary mesopores. This would enable the synthesis of NCs with hierarchical porosity, which can ultimately lead to more robust systems for acetylene hydrochlorination.

Herein, we develop a salt template-assisted chemical blowing approach,[9] employing NH_4Cl as a blowing agent, hexamethylene tetraamine (HMT) as the C/N-precursor, and Mg $(OAc)_2$ or $CaCO_3$ as thermally decomposable templates (Fig-

[a] S. K. Kaiser, Dr. S. Mitchell, Prof. J. Pérez-Ramírez
Institute for Chemical and Bioengineering
Department of Chemistry and Applied Biosciences
ETH Zurich
Vladimir-Prelog-Weg 1
Zurich 8093 (Switzerland)
E-mail: jpr@chem.ethz.ch
[b] K. S. Song, Prof. A. Coskun
Department of Chemistry
University of Fribourg
Chemin de Musée 9
Fribourg 1700 (Switzerland)
E-mail: ali.coskun@unifr.ch

Supporting information for this article is available

ure 1, see Supporting Information for experimental details) to tune the porosity of NCs, with controllable N-content and speciation, and to systematically assess their stability in acetylene hydrochlorination. Since the carbonization temperature (T_C) contributes significantly to the development of the porous properties and nitrogen functionalities, we initially studied this key parameter with the non-templated NC-I in the range of 773–1273 K (Figures S2-4). In good agreement with existing literature,[3b,4b,f,10] NCs carbonized at T_C = 973-1173 K exhibit the highest initial activity in acetylene hydrochlorination (Figure S4). This has been ascribed to an interplay of catalytic descriptors, including a high content of pyridinic and pyrrolic nitrogen sites and a moderate concentration of surface defects in the carbon structure, associated with good electrical conductivity, which possibly facilitates surface diffusion of reactants and intermediates.[4f] To increase the micropore volume of NC-I without changing the optimized nitrogen speciation, we fixed the carbonization temperature to 973 K and employed the decomposable templates ($Mg(OAc)_2$ or $CaCO_3$) to boost the chemical blowing effect. Thermogravimetric analysis coupled with differential scanning calorimetry (TGA/DSC) in Ar atmosphere was used to mimic the carbonization process of the NC series, monitoring the gas evolution by mass spectrometry (MS, Figure S5). Particularly H_2O and CO_2 are released in an endothermic process during the synthesis of NC-II and NC-III, which is not observed for NC-I. Notably, the relative distribution of the nitrogen functionalities and the total N-content, as derived from N 1s XPS and elemental analysis, as well as the carbon structure and concentration of surface defects, as analyzed by Raman spectroscopy, remain relatively unaffected by the addition of the salt-template precursors in the NC synthesis (Tables 1, S1, S2, Figures 2a, S11). In stark contrast, the surface area and the pore volume increased by 2 and 4 times for NC-II and NC-III, respectively, in comparison to NC-I (Table 1, Figure 2b). In line with this finding, the acetylene adsorption capacity also follows the same trend (Figures 2c, S6). Besides the significantly enhanced microporosity, NC-II and NC-III also exhibit additional meso- and macropores due to the addition of salt-templates in their synthesis, as verified by scanning transmission electron microscopy (STEM) images (Figures 2d, S7, S8). This observation supports the *in-situ* formation of the metal oxides and chlorides (*i.e.*, $MgO/MgCl_2$ and $CaO/CaCl_2$ Figure S5) during the carbonization process to serve as salt templates for the generation of additional pore networks.

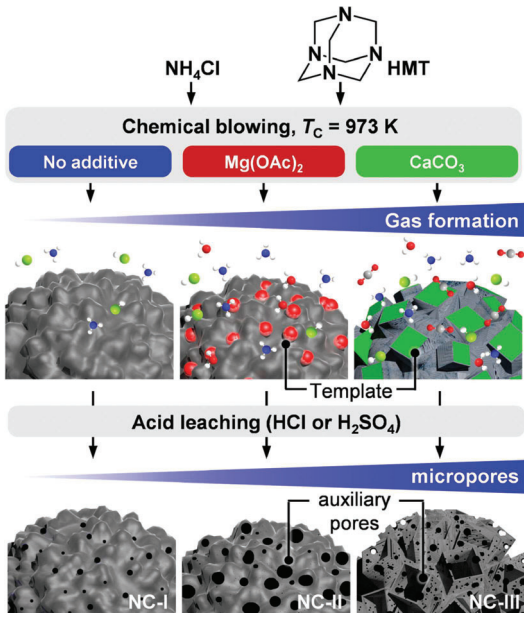

Figure 1. Synthetic steps involved in the preparation of NCs with varying textural properties at a fixed N-content and speciation. Color-code: N: blue, Cl: green, O: red, C: grey.

Table 1. Characterization data of fresh and used NC catalysts.

Catalyst	N[a] [wt.%]	C[a] [wt.%]	Cl[a] [wt.%]	V_{total}[b] [$cm^3 g^{-1}$]	V_{micro}[c] [$cm^3 g^{-1}$]	S_{BET}[d] [$m^2 g^{-1}$]
NC-I	17.0	71.5	0.0	0.10	0.06	245
NC-II	15.0	58.7	0.1	0.29	0.22	643
NC-III	17.0	55.9	0.2	0.70	0.42	1290
NC-I-12 h	15.5	71.4	5.3	0.00	0.00	6
NC-II-12 h	15.0	59.3	5.5	0.15	0.10	326
NC-III-12 h	15.7	56.8	5.4	0.36	0.25	734
NC-II-30 h	15.2	66.5	6.3	0.00	0.00	19
NC-III-30 h	17.0	60.2	5.6	0.33	0.21	633
NC-II-60 h	15.4	71.0	5.6	0.00	0.00	1
NC-III-60 h	16.2	65.1	6.5	0.24	0.15	451

[a] Elemental analysis, [b] Volume of Ar adsorbed at $p/p_0 = 0.98$, [c] *t*-plot method, [d] BET method.

To study the effect of porosity on the performance of NCs in acetylene hydrochlorination, we conducted 12–60 h tests with the NC series under accelerated deactivation conditions, applying a high gas hourly space velocity based on acetylene (*GHSV*(C_2H_2), of 650 h^{-1}) at an optimized reaction temperature of T_{bed} = 523 K (Figures 3, S6, S9, Table S3). While NC-I and NC-II exhibit a similar initial activity (Y_0(VCM) = 60 %), NC-III is less active (Y_0(VCM) = 35 %). This observation indicates an upper threshold to the previously reported positive correlation between enhanced porous properties and catalytic activity.[3b] Since the acetylene adsorption capacity is significantly enhanced for NC-III (Figure 2c), it is likely that also VCM adsorbs stronger over this catalyst compared to NC-I and NC-II. Consequently, the hampered desorption of VCM might account for the comparably lower activity of NC-III. As expected, NC-I rapidly deactivates with time-on-stream (*tos*, linearized deactivation constant k_D = 20 h^{-1}, derived *via* linear regression of the initial 5 h *tos*), at a rate slightly higher compared to benchmark polyaniline-derived N-doped carbon (NC, k_D = 14 h^{-1}, Figure S9).[4f] Remarkably, the stability of NC-II and NC-III is *ca.* 3 and 50 times improved (k_D = 7 h^{-1} and k_D = 0.3 h^{-1}), with respect to NC-I, indicating a superlinear correlation between catalyst lifetime and porous properties. To confirm this theory, we sampled the NC catalysts at different *tos* (12 h, 30 h, 60 h) for detailed characterization. Changes in the carbon structure and relative distribution of nitrogen functionalities could be excluded by Raman spectroscopy and N 1s XPS analysis (Figure S11). Elemental analysis and STEM elemental mapping evidence a rapid accumulation of chlorine-containing com-

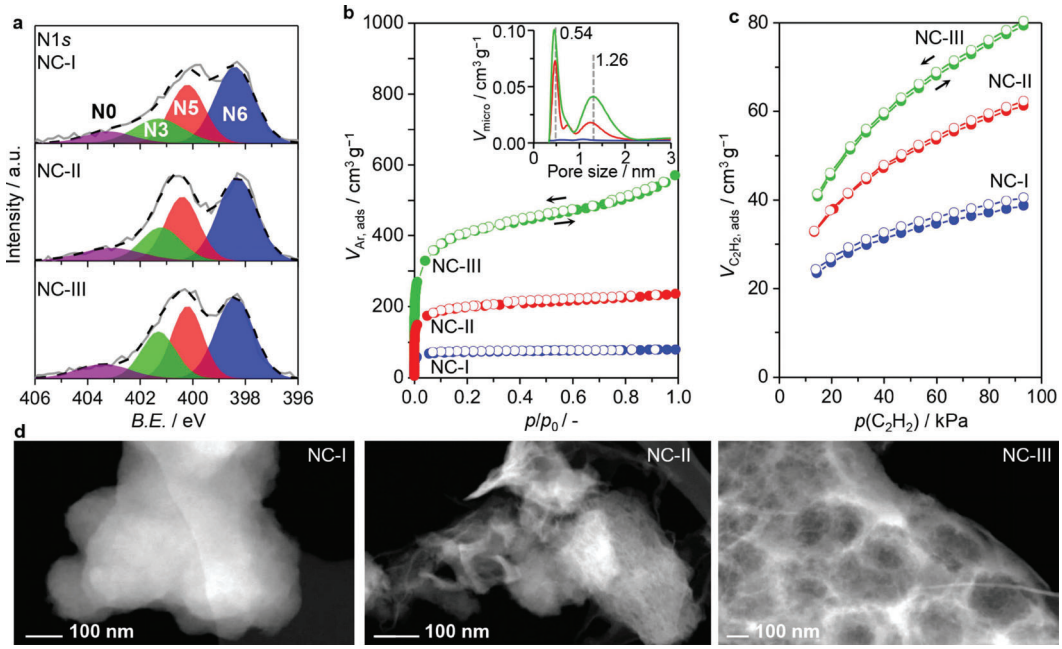

Figure 2. a, N 1s XPS spectra. **b**, Ar adsorption (filled) and desorption (open) isotherms of NC-I, -II, -III and their pore size distribution calculated *via* NLDFT method (inset). **c**, C_2H_2 chemisorption isotherms at 308 K. **d**, HAADF-STEM images.

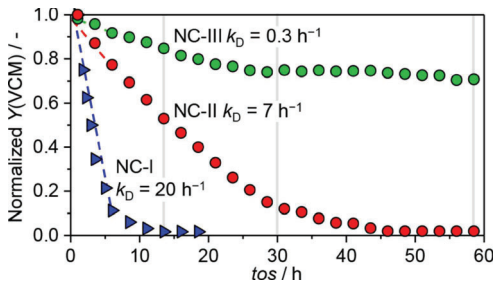

Figure 3. Time-on-stream (*tos*) performance of the NC series indicated as the normalized yield of vinyl chloride monomer (*Y*(VCM)). The deactivation constants, k_D, were derived *via* a simple linear regression of the data range indicated by the respective trend lines. Reaction conditions: $T_{bed} = 523$ K, $F_T = 15$ cm^3 min^{-1}, HCl:C_2H_2:Ar = 44:40:16, $W_{cat} = 0.25$ g, $P = 1$ bar. Initial yields of VCM, Y_0(VCM) = 62 %, 60 %, 35 % for NC-I, NC-II, and NC-III, respectively.

pounds within the initial 12 h *tos* (Figure S12). With proceeding reaction time (> 12 h), the total Cl-content remains relatively constant, indicating Cl-saturation. Interestingly, this behavior, including the rate of the Cl-uptake, is similar for all catalysts and hence does not correlate with their respective deactivation trends. On the contrary, the surface area and the pore volume gradually decrease for the whole NC series (Figure 4a–c), accompanied by an increase in carbon deposits, as determined by TGA-MS (Figure S10) and corroborated by elemental analysis (Table 1). In addition, the acetylene adsorption capacity, as derived from the temperature programmed desorption of acetylene (C_2H_2 TPD) gradually declines in the order of NC–I > NC–II > NC–III, (Figure 4d), which also agrees well with the respective deactivation rates. Overall, these observations suggest that the pore structure of NCs significantly affects their intrinsic stability in acetylene hydrochlorination. Particularly micropores are easily blocked, inhibiting effective acetylene adsorption and causing rapid catalyst deactivation (NC-I). On the contrary, the meso- and macropores do not show significant structural/morphology changes with increasing *tos*, as visualized by STEM analysis (NC-II, NC-III, Figure 4e), granting hierarchical NCs superior stability in acetylene hydrochlorination, reaching comparable levels to state-of-the-art precious metal-based catalysts (Table S3).

In conclusion, we have shown for the first time that employing decomposable salt templates, such as calcium carbonate and magnesium acetate, in the chemical blowing approach enables the facile synthesis of hierarchical nitrogen-doped carbons, with controllable N-content and speciation. The simultaneous increase in the micro- and mesopore volume is due to enhanced gas evolution through the reaction of the salt-template and the chemical blowing agent, while the *in-situ* formed metal oxides and chlorides (*i.e.*, MgO/$MgCl_2$ and CaO/$CaCl_2$) further serve as templates for the generation of additional meso- and macropores. Following this approach, we derived a series of NCs with varying porosity (*i.e.,* surface area, pore size and volume) at a fixed N-content and speciation, carbon structure and concentration of surface defects, which enabled us to decouple a complex interplay of catalytic descriptors and conduct the first systematic study of porosity effects on the stability of NCs in acetylene hydrochlorination. While micropores are easily blocked, inhibiting effective acetylene adsorption and causing rapid catalyst deactivation, meso- and macropores do not show significant structural/morphology changes under reaction conditions, enhancing the lifetime of hierarchical NCs by *ca.* 50 times compared to their

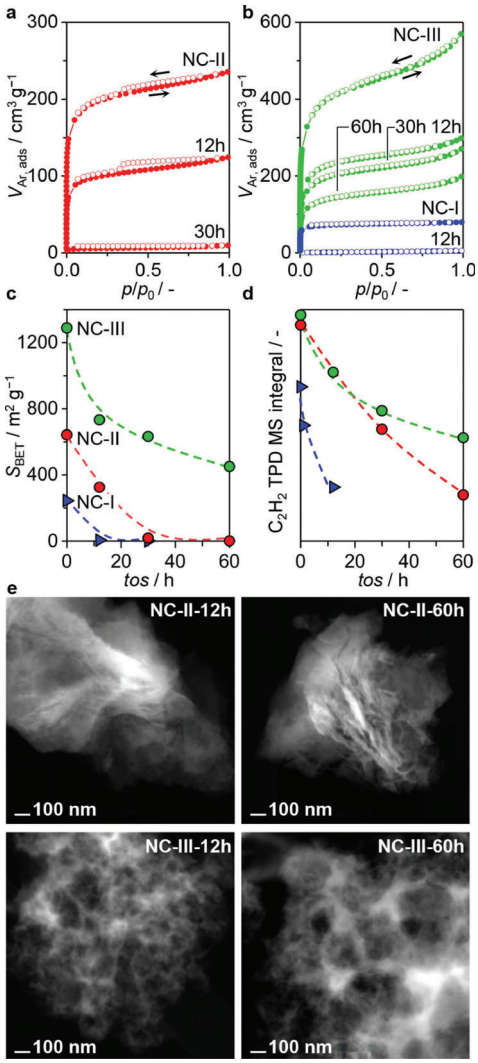

Figure 4. a, **b**, Ar isotherms of NCs after varying time-on-stream. **c**, decrease in surface area with increasing *tos*. **d**, C_2H_2 uptake of the fresh (colored) and used (black) NC catalysts and amount of coke in the used catalysts, as derived by TGA-MS analysis. **e**, Filtered HAADF-STEM images of the NC-III catalyst after 12 h and 60 h in acetylene hydrochlorination.

pristine microporous analogues. These results evidence a tremendous impact of porosity, encompassing improved pore accessibility and molecular transport, on the stability of metal-free hydrochlorination catalysts, which serves as an important guideline for future research in this field. In particular, dedicated diffusion experiments will be valuable to further direct catalyst design and to establish a direct correlation between lifetime and porosity *via* improved diffusivity in the hierarchical N-doped carbons.

Experimental Section

Full experimental details as well as additional characterization and catalytic data are provided in the Supporting Information.

Acknowledgements

This work was supported by ETH research grant (ETH-40 17-1) and the Swiss National Science Foundation (project no. 200021-175947). We thank Pierre Mettraux for conducting the XPS analysis. The Scientific Centre for Optical and Electron Microscopy (ScopeM) at ETH Zurich is acknowledged for the use of their facilities.

Keywords: acetylene hydrochlorination · catalyst stability · hierarchical porosity · N-doped carbon · chemical blowing

[1] a) D. S. Su, J. Zhang, B. Frank, A. Thomas, X. Wang, J. Paraknowitsch, R. Schlögl, *ChemSusChem* **2010**, *3*, 169–180; b) L. Dai, Y. Xue, L. Qu, H. J. Choi, J. B. Baek, *Chem. Rev.* **2015**, *115*, 4823–4892; c) X. Liu, L. Dai, *Nat. Rev. Mater.* **2016**, *1*; d) Y. Zeng, R. Zou, Y. Zhao, *Adv. Mater.* **2016**, *28*, 2855–2873; e) L. Dai, *Carbon-Based Metal-Free Catalysts: Design and Applications, Vol. 2*, John Wiley & Sons, **2018**, pp. 167–218; f) G. Singh, I. S. Ismail, C. Bilen, D. Shanbhag, C. I. Sathish, K. Ramadass, A. Vinu, *Appl. Energy* **2019**, *255*, 113831.

[2] a) G. Lan, Y. Qiu, J. Fan, X. Wang, H. Tang, W. Han, H. Liu, H. Liu, S. Song, Y. Li, *Chem. Commun.* **2019**, *55*, 1430–1433; b) Y. Qiu, S. Ali, G. Lan, H. Tong, J. Fan, H. Liu, B. Li, W. Han, H. Tang, H. Liu, Y. Li, *Carbon* **2019**, *146*, 406–412.

[3] a) X. Li, Y. Wang, L. Kang, M. Zhu, B. Dai, *J. Catal.* **2014**, *311*, 288–294; b) X. Qiao, Z. Zhou, X. Liu, C. Zhao, Q. Guan, W. Li, *Catal. Sci. Technol.* **2019**, *9*, 3753–3762.

[4] a) B. Dai, K. Chen, Y. Wang, L. Kang, M. Zhu, *ACS Catal.* **2015**, *5*, 2541–2547; b) X. Li, J. Zhang, W. Li, *J. Ind. Eng. Chem.* **2016**, *44*, 146–154; c) Y. Yang, G. Lan, X. Wang, Y. Li, *Chin. J. Catal.* **2016**, *37*, 1242–1248; d) S. Chao, F. Zou, F. Wan, X. Dong, Y. Wang, Y. Wang, Q. Guan, G. Wang, W. Li, *Sci. Rep.* **2017**, *7*, 39789; e) X. Dong, S. Chao, F. Wan, Q. Guan, G. Wang, W. Li, *J. Catal.* **2018**, *359*, 161–170; f) R. Lin, S. K. Kaiser, R. Hauert, J. Pérez-Ramírez, *ACS Catal.* **2018**, *8*, 1114–1121; g) J. Zhao, B. Wang, Y. Yue, G. Sheng, H. Lai, S. Wang, L. Yu, Q. Zhang, F. Feng, Z.-T. Hu, X. Li, *J. Catal.* **2019**, *373*, 240–249.

[5] a) I. T. Trotus, T. Zimmermann, F. Schüth, *Chem. Rev.* **2014**, *114*, 1761–1782; b) P. Johnston, N. Carthey, G. J. Hutchings, *J. Am. Chem. Soc.* **2015**, *137*, 14548–14557; c) R. Lin, A. P. Amrute, J. Pérez-Ramírez, *Chem. Rev.* **2017**, *117*, 4182–4247; d) H. Xu, G. Luo, *J. Ind. Eng. Chem.* **2018**, *65*, 13–25; e) J. Zhong, Y. Xu, Z. Liu, *Green Chem.* **2018**, *20*, 2412–2427; f) S. K. Kaiser, R. Lin, F. Krumeich, O. V. Safonova, J. Pérez-Ramírez, *Angew. Chem. Int. Ed.* **2019**, *58*, 12297–12304; g) S. K. Kaiser, R. Lin, S. Mitchell, E. Fako, F. Krumeich, R. Hauert, O. V. Safonova, V. A. Kondratenko, E. V. Kondratenko, S. M. Collins, P. A. Midgley, N. López, J. Pérez-Ramírez, *Chem. Sci.* **2019**, *10*, 359–369.

[6] X. Li, P. Li, X. Pan, H. Ma, X. Bao, *Appl. Catal. B* **2017**, *210*, 116–120.

[7] a) X. Li, X. Pan, L. Yu, P. Ren, X. Wu, L. Sun, F. Jiao, X. Bao, *Nat. Commun.* **2014**, *5*, 3688; b) M. Zhu, Q. Wang, K. Chen, Y. Wang, C. Huang, H. Dai, F. Yu, L. Kang, B. Dai, *ACS Catal.* **2015**, *5*, 5306–5316.

[8] G. Lan, Y. Wang, Y. Qiu, X. Wang, J. Liang, W. Han, H. Tang, H. Liu, J. Liu, Y. Li, *Chem. Commun.* **2018**, *54*, 623–626.

[9] S. N. Talapaneni, J. H. Lee, S. H. Je, O. Buyukcakir, T.-w. Kwon, K. Polychronopoulou, J. W. Choi, A. Coskun, *Adv. Funct. Mater.* **2017**, *27*, 1604658.

[10] J. Wang, F. Zhao, C. Zhang, L. Kang, M. Zhu, *Appl. Catal. A* **2018**, *549*, 68–75.